Nonlinear Taylor Instability of a Plane Interface between Two Incompressible Fluids with Interfacial Mass Transfer

A principal mechanism for rapid mixing and fragmentation in vapor explosions, such as have occurred in the LNG, aluminum, steel and paper industries, is thought to be nonlinear Taylor instability. An analysis, based on a generalized coordinate method developed by Dienes for a fluid with an arbitrary constitutive law, is here extended to a two-fluid model, with or without mass transfer between the fluids. Numerical results indicate that in a steam-water system entrainment starts in times of order 10^{-4}s at 100 G acceleration normal to the interface. For gas-liquid systems the presence of the second fluid changes the instability growth only slightly. Condensation of steam, even when limited only by the kinetic theory interfacial resistance, also has minor effects on the growth rate. However, condensation on the entrained drops will have a major effect on the acceleration.

I-HWA M. CHANG and S. G. BANKOFF

Chemical Engineering Department
Northwestern University
Evanston, IL 60201

SCOPE

The formation of the well-known "spike and bubble" geometry due to nonlinear effects when an interface between two semi-infinite fluids is accelerated in a direction from the light into the heavier fluid, is of great practical importance. Rapid mixing of the two fluids ensues, which determines the fragmentation of water drops behind a shock front moving with a supersonic aircraft, entrainment of sodium droplets into an expanding gas mass in a hypothetical accident in the liquid-metal fast breeder reactor, and a host of other practical applications where rapid, small-scale mixing is a vital consideration. Progress in this area has been difficult, although the linear theory has been well-known for more than a century. Recently, however, a nonlinear theory due to Dienes (1978) which was based on earlier work by Fermi (1956) and by Miles and Dienes (1966), gives promise of analytical treatment of nonlinear instability problems involving a variety of practical complications, such as viscous and surface effects, and elastic-plastic deformation of a solid. The Dienes model concerned itself only with a single fluid lying in a semi-infinite half-space. In this work, motivated by the problem of condensation of steam at an accelerated water interface, we extend the Dienes theory to two-fluid interfaces with mass transfer.

CONCLUSIONS AND SIGNIFICANCE

It is shown that the effects of a vapor phase, with or without surface condensation, do not affect the character of the nonlinear Taylor instabilities in any important way. The present formulation predicts infinite spike velocities ($q = 1$) in very small times ($\sim 10^{-4}$s for 100 G). This agrees with the observations of Bankoff et al. (1982) in a steam-water shock tube. In actual practice the spikes will break up to give a succession of droplets which are dispersed into the vapor phase. One can thus expect very rapid condensation on these small drops, thereby decreasing the acceleration, and hence the work potential, of the liquid slug by a large factor (perhaps one or more orders of magnitude). This represents an important area for future work, both from a theoretical and practical point of view. The large decrease in work potential is an important finding for the safety of liquid-metal fast-breeder and light-water reactors.

If the second fluid is a liquid, the growth of the instability is significantly slower. Elastic-plastic deformations of solid crusts can also be handled by the Dienes theory. Hence, a number of applications of these results can be envisaged in rapid mixing in solid-liquid, liquid-liquid, and gas-liquid systems.

Finally, the influence of initial small surface perturbations, not only of surface velocity, $\dot{q}$, but of surface height, η, needs to be explored. The single-mode approximation can result in inconsistencies unless $k\eta_o \ll 1$.

INTRODUCTION

The stability of the interface between two semi-infinite inviscid and incompressible fluids, lying one above the other, was first investigated by Rayleigh (1900). There are two general approaches, both leading to the same results. One can assume a small traveling wave at the interface, and determine the conditions at which the wave speed (or frequency) become complex (Lamb, 1932), or one can assume a standing wave, which may grow or decay according to the solution of an initial-value problem. In either case one finds a time dependence of the form $\exp(nt)$, where $n = [g_o k(\rho_1 - \rho_2)/(\rho_1 + \rho_2)]^{1/2}$. Here g_o, the acceleration due to gravity, is taken to be positive, and ρ_1 and ρ_2 are the densities of the upper and lower fluids respectively. If $\rho_1 > \rho_2$, the wave is unstable. Taylor (1950), in connection with wartime studies of the expansion of the hot-air "bubble" produced by an atomic bomb, observed that this is equivalent to instability whenever an acceleration is imposed on the entire system directed from the light phase to the heavy phase.

Bellman and Pennington (1954), using an initial value analysis, found the effect of surface tension, σ, on the growth rate to be

$$n = \left[\frac{k(g + g_o)(\rho_1 - \rho_2)}{(\rho_1 + \rho_2)} - \frac{\sigma k^3}{(\rho_1 + \rho_2)}\right]^{1/2} \quad (1)$$

0001-1541-83-5842-0095-$2.00.

n is real when

$$k \leq \left[\frac{(g + g_o)(\rho_1 - \rho_2)}{\sigma}\right]^{1/2} = k_c \tag{2}$$

The most dangerous wave number, k_m, is found by setting $dn/dk = 0$, giving

$$k_m = \left[\frac{(g + g_o)(\rho_1 - \rho_2)}{3\sigma}\right]^{1/2} \tag{3}$$

By bounding the roots with a comparison equation they also arrived at an estimate of the damping factor due to viscosity on the growth rate. Bankoff (1955), using a complex potential formulation for an observer traveling with the wave (Milne-Thomson, 1955) later obtained, by an energy method, an identical result for the viscosity damping, except for a factor of $2^{1/3}$. A number of other results for combined Taylor and Helmholtz instability were given.

All of these theories are applicable for short times only. Lewis (1950), whose experimental results matched the initial amplitude growth rate predicted by Taylor, observed that the growth rate changed when the amplitude grew to a size on the order of 0.4 λ, where λ is the disturbance wavelength. Lewis noted that beyond this amplitude the denser fluid will form narrow spikes into the lighter fluid, while the lighter fluid forms bubbles that move into the denser fluid.

Fermi (1956), by grossly schematizing the shape of the wave into a rectangular shape, and using a rough energy balance (kinetic and potential) for the period subsequent to the breakdown of the exponential amplitude growth, was able to demonstrate that the half wave of the heavy liquid moving into the vacuum becomes rapidly narrower, whereas the half wave pushing into the heavy liquid becomes more and more blunt. On the other hand, he failed to account for the experimental results according to which the front of the wave pushing into the heavy liquid moves with constant velocity. In the nonlinear final growth stage, Emmons, et al. (1960) observed a constant-velocity growth of the amplitude, and correlated it with a Taylor bubble rise velocity, as did also Lewis:

$$V_r = C\sqrt{g\lambda_o} \tag{4}$$

where λ_o is the experimentally observed wavelength. Lewis reported the constant C to be 0.78 and Emmons 0.3. No reason for the disparity was noted, although it was emphasized that the scatter in the data was large.

Daly (1969), incorporating the effect of surface tension, made use of the two-fluid version of the marker-and-cell technique for time-dependent incompressible flow studies. For at least the early stages of Rayleigh-Taylor instability, the numerical techniques predicted growth rates in good agreement with the linear analysis of Chandrasekhar (1961).

Corradini (1978) undertook an experimental study with the purpose of predicting the entrainment observed during a transient expansion of a vapor source into a liquid pool. The final stage growth appears to be the dominant growth for long times and thus useful in entrainment modeling. The ratios of k_c/k and g/g_o investigated in previous experimental studies were small in comparison to those that may appear in a large scale system. Therefore, his experiment was performed at $100 < g/g_o < 1{,}000$ and $k_c/k > 10$, using an experimental design similar to that of Lewis. The initial wavelength is controlled by the speed of a motorized paddle. Not only did the initial wavelength begin to penetrate the surface but smaller wavelengths near the critical size also appeared and grew into the liquid. The main fluid pair used in the experiment was air-water. The relative penetration velocity was correlated by

$$v_b = 0.54g^{0.332\pm0.27} \tag{5}$$

with a large data spread.

Cagliostro et al. (1978) studied the effects of vessel internal structures on the work potential of hypothetical core disruptive accidents in a 1/30-scale model of a demonstration size liquid-metal fast breeder reactor. Their conclusion was that Taylor instability appears to be the dominant mechanism for coolant entrainment.

Christopher and Theofanous (1977) investigated the transient development of air discharges into a liquid pool without the prototypic thermal effects present during core disruptive accidents. The initial discharge grew as a smooth hemispherical bubble with a preferred growth in the vertical direction while the pool upper surface accelerated uniformly. The bubble expanded to the vessel wall in 7 to 8 ms. After reaching the wall, the bubble expanded essentially in a one-dimensional fashion. Visually, reversal of the pool acceleration was marked by the onset of Taylor instability at the upper surface at 21 ms. The instability is clearly seen in the upper pool interface of all the runs as the pool decelerates. The pool pressure became less than the expansion plenum pressure at approximately 13 ms, indicating that the pool was decelerating. Consequently, the approximate time necessary for the instability to develop to an observable magnitude was 8 ms. The absence of Taylor (exponential) instability is characteristic of spherical bubble growth. In these experiments the acceleration had become small by the time the flow became parallel to the vessel walls.

Dienes (1978) extended previous developments by Fermi (1956) and by Miles and Dienes (1966) on nonlinear Taylor instability, employing a Lagrangian formulation of the equations of motion, with generalized coordinates consisting of the time-dependent amplitude functions of the Fourier expansion of the surface perturbation of a single semi-infinite fluid. An energy method is used to generate a set of nonlinear differential equations for the generalized coordinates. In practice only the dominant wavelength is used, so that only one nonlinear equation needs to be solved. The characteristic bubble-and-spike shape is obtained, with the spike amplitude becoming infinite at a finite time. The great advantage of the energy method is that it allows viscous and surface tension effects to be incorporated easily, as well as elastic and plastic deformation energies if the "fluid" region consists partly or completely of a freezing or frozen liquid. Dienes and Cooper (1978) applied this method to the UO_2-sodium system, and concluded the effect of solidification was minor, since the rate of crust growth was too small to influence the Taylor instability markedly. However, Sharon and Bankoff (1979) noted that with different assumptions, the solidification effect could become dominant. In the Dienes-Cooper analysis, solidification and acceleration begin at the same instant. The Sharon-Bankoff analysis assumes a hydrodynamic premixing time, in which the two liquids are separated by a vapor film. This time, of the order of fraction of a second to seconds, is required to produce a large-scale explosion over a significant fraction of the reactor fuel inventory. Heat transfer during this premixing time, prior to the triggering event in the form of a pressure shock wave which collapses the vapor blankets, can result in sufficient crust thickness to resist fracture by Taylor instability.

DEVELOPMENT OF A TWO-FLUID MODEL

We consider now the case of two incompressible and immiscible fluids lying one above the other. The heavier fluid, of density ρ_1, occupies the region $-\infty \leqq x \leqq \infty, 0 \leqq y \leqq h_1$, while the lighter fluid of density ρ_2, occupies the region $-\infty \leqq x \leqq \infty, -h_2 \leqq y \leqq 0$. Two-dimensional flow is considered, as is customary in Taylor instability analyses. The system is subjected to an effective gravity force, $g(t)$, downwards, which is, in general, time-dependent, but is here considered to be a constant. The assumption is now made that the flow fields can be described by the velocity potentials

$$\phi_j(x,y,t) = Re\left[\frac{1}{2\pi}\int \exp(ikx + (-1)^j ky)\tilde{\phi}_j(k,t)dk\right]_{j=1,2} \tag{6}$$

This implies that h_1 and h_2 are taken sufficiently large to have negligible effect on the interfacial motion, and that viscous effects are confined to a very thin boundary layer on both sides of the interface, which is of negligible thickness during the time scales of interest. During the linear growth period the integral is rapidly dominated by the fastest-growing wavenumber, k_o, and the assumption is made here that this wavenumber remains dominant

and constant during the nonlinear growth period. The simplification is thus made that the velocity potentials are given by

$$\phi_1 = \dot{q}_{ko}(t)\cos(k_o x)\exp(-k_o y)/k_0^2 \quad y \geq 0 \tag{7}$$

$$\phi_2 = -\dot{q}_{ko}(t)\cos(k_o x)\exp(k_o y)/k_0^2 \quad y \leq 0 \tag{8}$$

These satisfy the Laplace equation, as required for incompressible inviscid fluids, and vanish at large distance from the interface. Essentially this is equivalent to the application of the method of steepest descent to the integrals in Eq. 6. The subscript will henceforth be dropped from k_o. One now obtains

$$v_{x1} = \frac{\dot{q}}{k}\sin(kx)e^{-ky};\quad v_{y1} = \frac{\dot{q}}{k}\cos(kx)e^{-ky} \tag{9}$$

$$v_{x2} = -\frac{\dot{q}}{k}\sin(kx)e^{ky};\quad v_{y2} = \frac{\dot{q}}{k}\cos(kx)e^{ky} \tag{10}$$

The particle path slope can be obtained from

$$\frac{dy_j}{dx_j} = \frac{v_{yj}}{v_{xy}} = (-1)^{j-1}\frac{\cos(kx)}{\sin(kx)};\quad j = 1,2 \tag{11}$$

where again 1,2 refer to the heavy and light fluids, respectively.

Using now subscripts to denote the position of a particle in the jth fluid (x_j,y_j), this is obtained in terms of its initial position (x_{oj},y_{oj}) by integrating Eqs. 9–11:

$$y_j = y_{oj} + \int_{x_{oj}}^{x_j}\frac{dy_j}{dx_j}dx_j = y_{oj} + \frac{(-1)^{j-1}}{k}ln\left(\frac{\sin kx_j}{\sin kx_{oj}}\right) \tag{12}$$

$$x_j = x_{oj} + \int_0^t v_{xj}dt =$$

$$x_{oj} + \frac{(-1)^{j-1}}{k}[q(t) - q_0]\sin kx_{oj}e^{(-1)^j k y_{oj}} \tag{13}$$

where $q(0) = q_o$. At the interface $y_{01} = y_{02}$ initially, and the interface is then described by

$$\eta(x,t) = \eta_o + \frac{1}{k}ln\left(\frac{\sin kx_1}{\sin kx_{o1}}\right) \tag{14}$$

with

$$x_1 = x_{o1} + \frac{q'}{k}\sin kx_{o1}e^{-k\eta_0} \tag{15}$$

where $k\eta(x,0) = k\eta_o \ll 1$ for all x (small initial perturbation), and where $q' = q - q_o$. Upon expanding, and taking $\exp[-k\eta_o] \sim 1$, one obtains

$$\sin kx_1 = \sin kx_{o1} + q'\sin kx_{o1}\cos kx_{o1} \tag{16}$$

which, on substitution into Eq. 14, gives

$$\eta(x,t) = \eta_o + \frac{1}{k}ln(1 + q\cos kx) \tag{17}$$

The subscript on x_o has been dropped, since for $x_{o1} = x_{o2}$, and a sufficiently small initial surface wave, $x_1 = x_2$, to the present order of approximation. The dimensionless quantity q can be looked upon as a generalized coordinate, representing the first Fourier coefficient in the wavenumber expansion of the integral in Eq. 6. For the present problem $0 \leq q(t) \leq 1$, and $q(t) = 1$ represents a singularity at $kx = \pi$, corresponding to the spike of the well-known "spike-and-bubble" configuration. The bubble vertex is at $kx = 0$, with the dimensionless wavelength being 2π.

Having obtained these results by purely kinematic considerations, it remains to determine the differential equation satisfied by $q(t)$ from an energy integral. An energy balance over one wavelength, in the absence of mass transfer, requires that

$$\sum_j \frac{d}{dt}\left\{\int_{V_j}\left[\frac{\rho_j}{2}(v_{xj}^2 + v_{yj}^2) + \rho_j g y_j\right]dV_j + \sigma\left[\int_0^\lambda\left[1 + \left(\frac{\partial\eta}{\partial x}\right)^2\right]^{1/2}dx - \lambda\right]\right\} = -2\mu_j\int_{V_j}(v_{i,k}v_{i,k})_j dV_j \tag{18}$$

where the summation convention is employed in the right-hand integral, with (i,k) taking the meanings (x,y), the comma representing differentiation, and $j = 1,2$ referring to the heavy and light fluids. Here

$$\int_{V_1}dV_1 = \int_0^\lambda dx\int_{\eta(x,t)}^{h_1}dy_1,$$

$$\int_{V_2}dV_2 = \int_0^\lambda dx\int_{-h_2}^{\eta(x,t)}dy_2$$

Equation 18 states that the rate of change of kinetic, potential, and surface energy is balanced by viscous dissipation. Upon making the appropriate substitutions, one eventually obtains the nonlinear equation for q

$$\frac{d}{dt}\left[\rho_1\dot{q}^2\frac{\pi}{2k^4(1-q^2)^{3/2}}\right] - \frac{\rho_1 g\dot{q}F(q)}{2k^3} + \frac{4\sigma}{k}\dot{q}K(q) + \frac{4\pi\rho_1\nu_1\dot{q}^2}{k^2(1-q^2)^{3/2}} + \frac{d}{dt}\left[\frac{\rho_2\dot{q}^2\pi}{4k^4}(2+q^2)\right] + \frac{\rho_2 g\dot{q}F(q)}{2k^3} + \frac{2\rho_2\nu_2\dot{q}^2\pi}{k^2}(2+q^2) = 0 \tag{19}$$

or, on collecting terms

$$\ddot{q}\left[\frac{\rho_2}{\rho_1} + (1-q^2)^{-3/2} + \frac{\rho_2}{2\rho_1}q^2\right] + \dot{q}\left[4\nu_1 k^2(1-q^2)^{-3/2} + 2\frac{\rho_2}{\rho_1}\nu_2 k^2(2+q^2) + \frac{\rho_2}{2\rho_1}q\dot{q} + \frac{3}{2}q\dot{q}(1-q^2)^{-5/2}\right] + \left(\frac{\rho_2}{\rho_1} - 1\right)\frac{gkF(q)}{2\pi} + \frac{4\sigma k^3}{\pi\rho_1}K(q) = 0 \tag{20}$$

where

$$F(q) = 4\int_0^\pi \frac{ln(1 + q\cos\theta)\cos\theta d\theta}{(1 + q\cos\theta)} \tag{21}$$

$$K(q) = \frac{q}{2}\int_0^\pi \frac{\sin^2\theta d\theta}{(1 + q\cos\theta)^2(1 + 2q\cos\theta + q^2)^{1/2}} \tag{22}$$

The linearized form of Eq. 20 is

$$\ddot{q}\left(\frac{\rho_2}{\rho_1} + 1\right) + \dot{q}\left(4\nu_1 k^2 + 4\frac{\rho_2}{\rho_1}\nu_2 k^2\right) + \left(\frac{\rho_2}{\rho_1} - 1\right)gkq + \frac{\sigma k^3 q}{\rho_1} = 0 \tag{23}$$

Taking $q = A\exp(nt)$, the linear growth constant is

$$n = \left[4k^2\frac{(\mu_1 + \mu_2)^2}{(\rho_1 + \rho_2)^2} + \frac{(\rho_1 - \rho_2)gk - \sigma k^3}{(\rho_1 + \rho_2)}\right]^{1/2} - 2k^2\frac{(\mu_1 + \mu_2)}{(\rho_1 + \rho_2)} \tag{24}$$

Upon setting $\mu_2 = \rho_2 = 0$, the single-fluid expressions are recovered. To analyze the behavior of Eq. 20, let

$$\text{the dimensionless wavenumber } l \equiv k/\beta,\ \beta \equiv \left[\frac{(\rho_1 + \rho_2)g}{\sigma}\right]^{1/2}$$

$$\zeta \equiv 4\frac{(\mu_1 + \mu_2)^2}{(\rho_1 + \rho_2)^2}\left[\frac{g(\rho_1 + \rho_2)^3}{\sigma^3}\right]^{1/2} \tag{25}$$

and

$$\theta \equiv (\rho_1 - \rho_2)/(\rho_1 + \rho_2)$$

In terms of these parameters,

$$n = 2\beta^2\frac{(\mu_1 + \mu_2)}{(\rho_1 + \rho_2)}\left[\left(l^4 + \frac{\theta l}{\zeta} - \frac{l^3}{\zeta}\right)^{1/2} - l^2\right] \tag{26}$$

Setting $dn/dl = 0$, the fastest-growing wavenumber is given implicitly by

$$\zeta = (\theta - 3l_m^2)^2/8(\theta + l_m^2)l_m^3 \tag{27}$$

$$\text{Defining } \hat{l}_m = l_m\theta^{-1/2},\ \hat{\zeta} = \zeta\theta^{1/2}$$

Eq. 27 becomes

$$\hat{\zeta} = (1 - 3\hat{l}_m^2)^2/8(1 + \hat{l}_m^2)\hat{l}_m^3$$

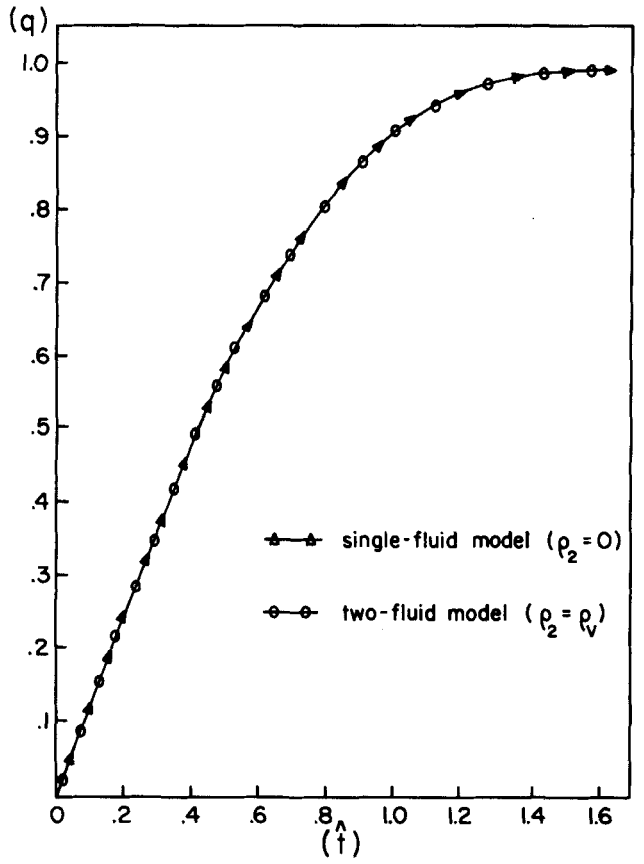

Figure 1. q vs. $\hat{t}$ at $k = k_m$ for steam-water.

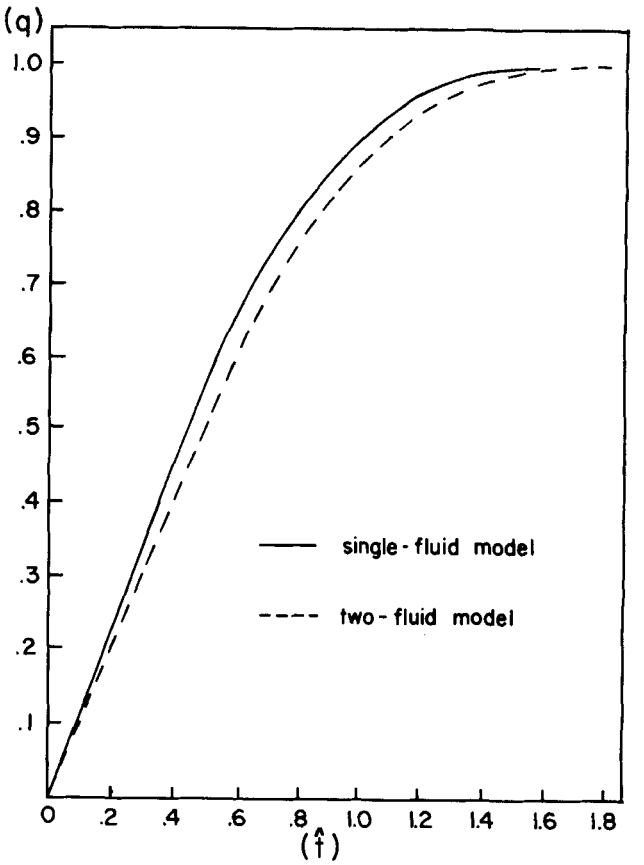

Figure 2. q vs. $\hat{t}$ at $k = k_m$ for mercury-water.

which is the form obtained by Dienes for a single fluid. Equation 20 can be converted to a nondimensional form by using:

$$\dot{Q} = \left(\frac{\sigma}{g^3\rho_1}\right)^{1/4}\dot{q}, \quad \zeta_1 = \nu_1^2\left(\frac{g\rho_1^3}{\sigma^3}\right)^{1/2}, \quad \hat{\rho} = \frac{\rho_2}{\rho_1}, \quad B_0 = \frac{\rho_1 g}{\sigma k^2}$$

$$\ddot{Q} = \left(\frac{\sigma}{g^3\rho_1}\right)^{1/2}\ddot{q}, \quad \zeta_2 = \nu_2^2\left(\frac{g\rho_1^3}{\sigma^3}\right)^{1/2}, \quad \hat{t} = \left(\frac{g^3\rho_1}{\sigma}\right)^{1/4} t \quad (28)$$

Equation 20 is thus transformed to:

$$\ddot{Q}\left[\hat{\rho} + (1-q^2)^{-3/2} + \frac{1}{2}\hat{\rho}q^2\right] + \dot{Q}\left[\frac{4\zeta_1^{1/2}}{B_0(1-q^2)^{3/2}} + \frac{2\hat{\rho}\zeta_2^{1/2}(2+q^2)}{B_0} + \frac{1}{2}\hat{\rho}q\dot{Q} + \frac{3}{2}\dot{Q}q(1-q^2)^{-5/2}\right] + \frac{(\hat{\rho}-1)F(q)}{2\pi B_0^{1/2}} + \frac{4K(q)}{\pi B_0^{3/2}} = 0 \quad (29)$$

Effect of Interfacial Mass Transfer

We consider here the case in which condensation of vapor at the interface is limited only by the kinetic theory interfacial resistance. In actual practice one can expect lower rates, due to the development of a thermal boundary in the liquid, and possibly to the development of a non-condensible gas concentration boundary layer on the vapor side of the interface. Thermocapillary effects are not considered here, although under some circumstances it is thought that they may be significant. A more detailed analysis would be required to take them into account. The energy balance then contains only one additional term, due to the kinetic energy of the condensate entering the interface. This is given by

$$\int_0^{\lambda}\frac{\dot{m}v^2}{2}\left[1+\left(\frac{\partial\eta}{\partial x}\right)^2\right]^{1/2}dx = \frac{\dot{m}^3}{4\rho_1^2 k} \times \int_0^{\pi}\frac{(1+2q\cos\theta+q^2)^{1/2}}{1+q\cos\theta}d\theta = \frac{\dot{m}^3}{4\rho_1^2 k}H(q) \quad (30)$$

Upon rearranging, the new differential equation for q is:

$$\ddot{q}\dot{q}\left[\frac{\rho_2}{\rho_1} + (1-q^2)^{-3/2} + \frac{\rho_2}{2\rho_1}q^2\right] + \dot{q}^2\left[4\nu_1 k^2(1-q^2)^{-3/2} + 2\nu_2\frac{\rho_2}{\rho_1}k^2(2+q^2)\right] + \dot{q}^3\left[\frac{3}{2}q(1-q^2)^{5/2} + \frac{\rho_2}{2\rho_1}q\right] + \dot{q}\left[\left(\frac{\rho_2}{\rho_1}-1\right)\frac{kgF(q)}{2\pi} + \frac{4\sigma k^3 K(q)}{\pi\rho_1}\right] + \frac{\dot{m}^3k^3H(q)}{4\rho_1^3} = 0 \quad (31)$$

This assumes that the liquid is well below the saturation temperature, so that its vapor pressure is negligible, and that turbulent mixing keeps the interfacial temperature close to the bulk liquid temperature. The change in the surface elevation due to the added volume of condensate has also been neglected.

NUMERICAL RESULTS AND DISCUSSION

We begin with the steam and water system at 107°C and 1.28 atm for the single-fluid model ($\rho_2 = 0$). The fastest-growing wavenumbers, based on the deep-water approximation, Eq. 27 is then a function of acceleration, as shown below

$g(\mathrm{m/s^2})$	$k_m(\mathrm{m^{-1}})$
9.8	238
98	754
980	2,384

$\dot{q}_o$ is chosen by setting the dimensionless parameter, $\dot{Q}$ as in Eq. 28, to 1.2 arbitrarily. Therefore, once g is fixed, both k_m and the initial velocity perturbation, $\dot{q}_o$, are also fixed. Figure 1 shows the solution from a numerical integration of Eq. 20 with ρ_2 set to zero for q vs. $\hat{t}$. An increase in g from 9.8 to 980 m/s^2 does not change the value of $\hat{t}$ at which q goes to one, but this represents a decrease in real time from 2.55×10^{-2} to 8.26×10^{-4}s. One sees that the onset of entrainment from a plane interface, or an interface subjected to large accelerations with essentially parallel motion,

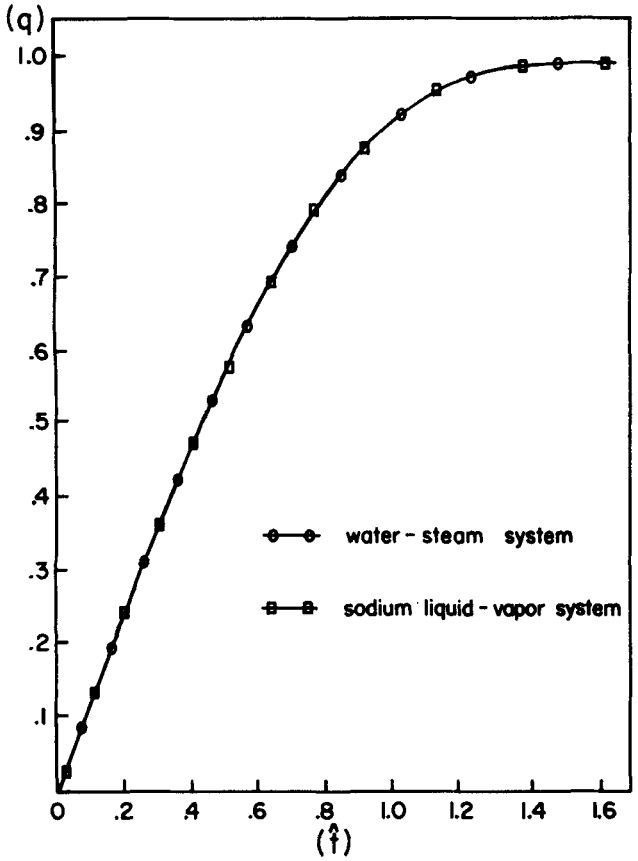

Figure 3. Condensation effect on q vs. $\hat{t}$ at $k = k_m$.

is very rapid. It is also seen from Figure 1 that the growth of the instability is not affected by taking $\rho_2 = 0$ (single-fluid model) or $\rho_2 = \rho_v$, the saturated vapor density of water at 107°C (two fluid model). However, Figure 2 shows significant density effects of the two fluid model on the growth of the instability with the mercury water system. Figure 3 shows the effect of steam condensation (Eq. 31). Using an accommodation coefficient $\sigma = 0.1$, the condensation flux, $\dot{m}$, is found to be 19.6 kg/m²·s. The numerical results show the change of the curve of q vs. $\hat{t}$ cannot be distinguished visually at these mass fluxes. Hence the instability at fixed acceleration is well modeled by non-condensing systems. However, the condensation on entrained drops may greatly affect the pressure in the steam space and hence reduce the acceleration. This problem requires further study.

For completeness some sodium liquid-vapor calculations were performed at 927°C with $\sigma_c = 1$ and a condensation mass flux of 90.9 kg/m²·s. The results, shown in Figure 3, are of the same general form as with the steam-water system, indicating the relatively weak effect of surface tension in the nonlinear stages.

The effect of the perturbation of the dimensionless parameter, $\dot{Q}_o$, and hence $\dot{q}_o$, on the growth rate is shown in Figure 4. An increase in $\dot{Q}_o$ from .006 to 6.0 corresponds to the decrease in the value of $\hat{t}$ at which q goes to one from 9.8 to 0.4. This represents a decrease in real time from $\sim 10^{-3}$ s to $\sim 10^{-4}$ s for 100 G.

It has been shown that the effects of the second fluid, with or without surface condensation, do not affect the character of the nonlinear Taylor instabilities in any important way. The present formulation predicts infinite spike velocities ($q = 1$) in very small times ($\sim 10^{-4}$ s for 100 G). In actual practice the spikes will break up to give a succession of droplets which are dispersed into the vapor phase. One can thus expect very rapid condensation on these small drops, thereby decreasing the acceleration, and hence the work potential, of the liquid slug by a large factor (perhaps one or more orders of magnitude). This represents an important area for future work.

NOTATION

Bo = Bond number, Eq. 28
q = imposed acceleration
g_o = acceleration due to gravity
G = g/g_o, normalized acceleration
h = height of fluid layer
k = wave number
k_c = critical wave number, Eq. 2
k_m = most dangerous wave number, Eq. 3
l = dimensionless wave number, Eq. 25
$\dot{m}$ = condensation mass flux
n = linear growth constant, Eq. 24
q = generalized coordinate defined by Eqs. 7 and 8
q' = $q(t) - q(o)$
t = time

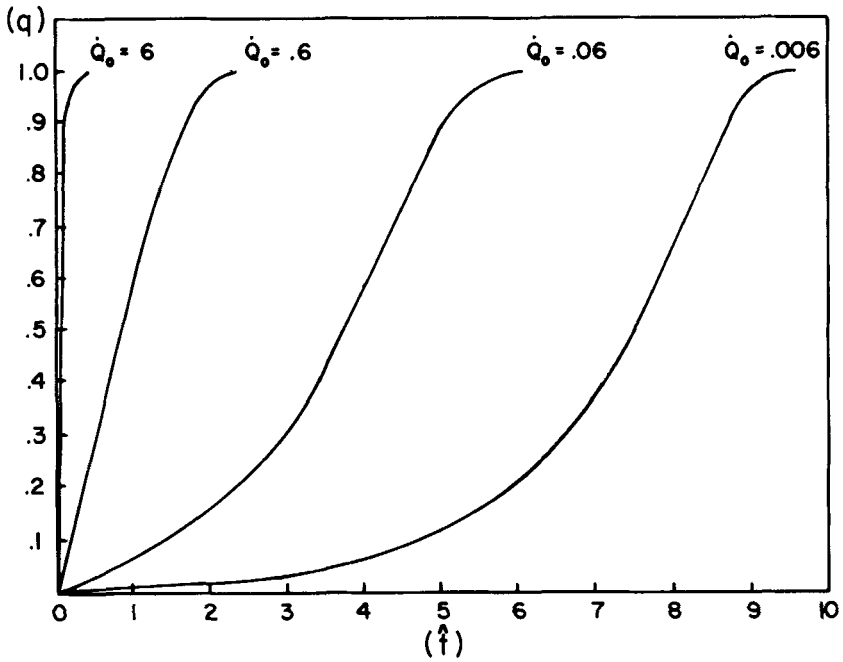

Figure 4. q vs. $\hat{t}$ at $k = k_m$ for steam-water at various $\dot{Q}_o$.

v_b = bubble penetration velocity
v_x, v_y = velocity components in x and y directions
x, y = Eulerian coordinates parallel and normal to undisturbed interface
x_o, y_o = Lagrangian coordinates marking a particular particle

Greek Letters

η = height of interface at (x,t)
η_o = initial height of interface at (x,o)
λ = wavelength
λ_o = experimentally observed wavelength
μ = viscosity
ν = kinematic viscosity
ρ = density
σ = surface tension
ϕ = velocity potential
ζ = dimensionless parameter, Eq. 25

Superscripts

$\hat{}$ = dimensionless variable, defined by Eq. 28

Subscripts

1 = heavy fluid
2 = light fluid
o = initial condition

LITERATURE CITED

Bankoff, S. G., and A. Sharon, "Modeling of Steady Plane Thermal Detonations," Proc. Int. Mtg. Fast Reactor Safety Technology, Seattle, WA, **5**, 1554 (1979).

Bankoff, S. G., G. Berthoud, J. M. Delhaye, and A. Pion, "Instabilités de Rayleigh-Taylor avec Condensation dans un Tube à Choc Eau-Vapeur," *Service des Transferts Thermiques*, Note T.T. 664, Centre des Études Nucléaires, Grenoble, France (1982).

Bellman, R. and R. H. Pennington, "Effects of Surface Tension and Viscosity on Taylor Instability," *J. of Applied Math.*, **12** (2), 153 (1954).

Chandrasekhar, S., *Hydrodynamics and Hydromagnetic Stability*, Oxford, Clarendon Press (1961).

Christopher, D. M., *Transient Development of a Two Phase Jet*, MS Thesis, Purdue University (1977).

Cooper, F. and J. Dienes, "The Role of Rayleigh-Taylor Instabilities in Fuel-Coolant Interactions," *Nuclear Science and Engineering*, **68**, 308 (1978).

Corradini, M. L., *Heat Transfer and Fluid Flow Aspects of Fuel-Coolant Interactions*, Ph.D. Thesis, Mass. Inst. of Technology (1978).

Daly, B. J., "Numerical Study of the Effect of Surface Tension on Interface Instability," *The Physics of Fluids*, **12**, 1340 (1969).

Dienes, J., "Method of Generalized Coordinates and An Application to Rayleigh-Taylor Instability," *The Physics of Fluids*, **21**, 736 (1978).

Emmons, H. W., C. T. Chang, and B. C. Watson, "Taylor Instability of Finite Surface Waves," *J. of Fluid Mechanics*, 177 (1960).

Fermi, E., "Taylor Instability of an Incompressible Liquid," in "Taylor Instability," Appendixes to Report LA-1862, LA-1927, Los Alamos Scientific Lab. (1956).

Ingraham, R. L., "Taylor Instability of the Interface Between Superposed Fluids—Solution by Successive Approximations," *Proc. Phys. Soc.*, London, **B67**, 748 (1954).

Lamb, H., *Hydrodynamics*, 6th ed., Dover, New York (1932).

Lewis, D. J., "The Instability of Liquid Surfaces When Accelerated in a Direction Perpendicular to Their Planes II," *Proc. Roy. Soc. Lond.*, **A202**, 81 (1950).

Miles, J. W., and J. K. Dienes, *The Physics of Fluids*, 9 (1966).

Milne-Thomson, K. M., *Theoretical Hydrodynamics*, 3rd ed., Macmillan Co., New York (1955).

Nayfeh, A. H., "On the Non-Linear Lamb-Taylor Instability," *J. of Fluid Mechanics*, **38**, 619 (1969).

Rayleigh, *Scientific Papers*, **ii**, Cambridge, England, 200 (1900).

Taylor, G., "The Instability of Liquid Surfaces When Accelerated in a Direction Perpendicular to Their Planes, I," *Proc. Roy. Soc., London*, **A201**, 192 (1950).

Tobin, R. J., and D. J. Cagliostro, "Effects of Vessel Internal Structures on Simulated HCDA Bubble Expansions," SRI Project PYU-3929, (1978).

Manuscript received December 14, 1981; revision received April 7, and accepted April 19, 1982.